Enhanced or suppressed six-wave mixing in a five-level atomic system*

Song Yue(宋 悦), Dai Guo-Xian(代国宪), Fu Yu-Xin(付雨欣),
Zhao Jin-Yan(赵金燕), Wang Zhi-Guo(王志国), and Zhang Yan-Peng(张彦鹏)†

Key Laboratory for Physical Electronics and Devices of the Ministry of Education and Shaanxi Key Laboratory of Information Photonic Technique, Xi'an Jiaotong University, Xi'an 710049, *China*

(Received 14 September 2010; revised manuscript received 3 December 2010)

We show the enhancement and suppression of a six-wave mixing (SWM) signal in the electromagnetically induced transparency in a five-level ^{85}Rb atomic system. The results show the Autler–Townes splitting and the enhancement or suppression of SWM, which are caused respectively by a self-dressing effect and by an external dressing effect in the presence of mutual dressing between two SWM signals. In addition, we observe the polarization dependence of the enhancement and suppression of the SWM signals.

Keywords: six-wave mixing, electromagnetically induced transparency, enhancement, suppression

PACS: 42.50.Gy **DOI:** 10.1088/1674-1056/20/7/074206

1. Introduction

In a multi-level system, the generated multi-wave mixing can be selectively enhanced or suppressed and the wave can be emitted with a small absorption under the electromagnetically induced transparency (EIT) conditions.[1−7] Such laser-induced atomic coherence has important influence on singly and doubly dressing schemes in multi-level systems.[8−11] On the other hand, when multi-Zeeman energy levels are involved in the atomic systems, polarizations of the involved laser beams can greatly influence the EIT and the six-wave mixing (SWM) processes.[12,13] In this paper, we show the enhancement and suppression of two coexisting SWM signals in the EIT window. More importantly, we report theoretical and experimental studies on the polarization dependence of the SWM processes and of the EIT profile.

2. Basic theory

This experiment is conducted in a ^{85}Rb vapor cell. The five energy levels (Fig. 1(a)) involved are $5S_{1/2}$ (F = 2, 3), $5P_{3/2}$ (F = 3), $5D_{3/2}$ and $5D_{5/2}$ (F = 2). The five laser beams are aligned spatially as shown in Fig. 1(b). The E_1 is a weak probe beam, whose wavelength is 780.245 nm. The E_1 propagates through the atomic medium and probes the transition from $|0\rangle$ to $|1\rangle$. Some significant parameters are wave vector k_i, frequency ω_i, Rabi frequency G_i and frequency detuning $\Delta_i = \Omega_i - \omega_i$, where Ω_i is the resonant frequency. The E_2, which drives the transition from $|1\rangle$ to $|2\rangle$, is a strong dressing laser beam with the wavelength of 775.978 nm propagating in the same direction as that of E_3. The E_3 and E_3' are the two pump beams, which share the same wavelength of 762 nm and propagate in the opposite direction with a small deviation angle $\sim$0.3°. They drive the transition from $|1\rangle$ to $|3\rangle$. The $E_{\rm F}$, which is a four-wave mixing (FWM) signal beam with the phase satisfying the condition $\boldsymbol{k}_{\rm F} = \boldsymbol{k}_1 + \boldsymbol{k}_3 - \boldsymbol{k}_3'$, is generated by E_1, E_3 and E_3'. The E_4 with the wavelength of 776.157 nm is another strong dressing laser beam driving the transition from $|1\rangle$ to $|4\rangle$. Therefore, there are two SWM signals, which are SWM1 satisfying the phase matching condition $\boldsymbol{k}_{\rm S1} = \boldsymbol{k}_1 + \boldsymbol{k}_3 - \boldsymbol{k}_3' + \boldsymbol{k}_2 - \boldsymbol{k}_2$ and SWM2 satisfying the phase matching condition $\boldsymbol{k}_{\rm S2} = \boldsymbol{k}_1 + \boldsymbol{k}_3 - \boldsymbol{k}_3' + \boldsymbol{k}_4 - \boldsymbol{k}_4$, respectively. These SWM signals form simultaneously and interact with each other. The FWM signals without the EIT window can be neglected. The generated FWM, SWM signals and the transmitted probe beam are detected

*Project supported by the National Natural Science Foundation of China (Grant Nos. 10974151, 61078002, and 61078020), the Program for New Century Excellent Talents in University of Ministry of Education of China (Grant No. 08-0431), and the Cross-Disciplinary Project of Xi'an Jiaotong University, China (Grant Nos. 2009xjtujc08, XJJ20100100, and XJJ20100151).

†Corresponding author. E-mail: ypzhang@mail.xjtu.edu.cn

© 2011 Chinese Physical Society and IOP Publishing Ltd

by an avalanche photodiode detector and a photodiode.

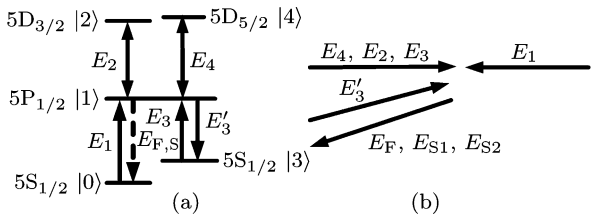


Fig. 1. (a) Relevant ^{85}Rb energy levels. (b) Spatial beam geometry used in the experiment.

Generally speaking, the expression of the SWM signal can be obtained by solving the coupled density-matrix equations under the circumstance of arbitrary intensity of incident laser field. Here, as the fields E_1 and E_3 are always quite weak, their dressing effect can be ignored. When the field E_2 is blocked, according to the perturbation chain $\rho_{00}^{(0)} \xrightarrow{\omega_1} \rho_{G_4\pm0}^{(1)} \xrightarrow{-\omega_3} \rho_{30}^{(2)} \xrightarrow{\omega_3} \rho_{G_4\pm0}^{(3)} \xrightarrow{\omega_4} \rho_{40}^{(4)} \xrightarrow{-\omega_4} \rho_{10}^{(5)}$, we can obtain $\rho_{10\mathrm{a}}^{(5)} = G_\mathrm{A}/[d_1 d_3 d_4 (d_1 + |G_4|^2/d_4)^2]$ for the SWM2 process, where $G_\mathrm{A} = \mathrm{i}\, G_1 G_3 G_3'^* G_4 G_4$, $d_1 = \mathrm{i}\,\Delta_1 + \Gamma_{10}$, $d_3 = \mathrm{i}(\Delta_1 - \Delta_3) + \Gamma_{30}$, $d_4 = \mathrm{i}(\Delta_1 + \Delta_4) + \Gamma_{40}$ and Γ_{ij} is the transverse relaxation rate between states $|i\rangle$ and $|j\rangle$. The intensity of SWM2 signal $I_\mathrm{SWM2} \propto |\rho_{10\mathrm{a}}^{(5)}|^2$. Similarly, when the field E_4 is blocked, according to another perturbation chain $\rho_{00}^{(0)} \xrightarrow{\omega_1} \rho_{G_2\pm0}^{(1)} \xrightarrow{\omega_2} \rho_{20}^{(2)} \xrightarrow{-\omega_2} \rho_{G_2\pm0}^{(3)} \xrightarrow{-\omega_3} \rho_{30}^{(4)} \xrightarrow{\omega_3} \rho_{10}^{(5)}$, $\rho_{10\mathrm{b}}^{(5)} = G_\mathrm{B}/[d_1 d_2 d_3 (d_1 + |G_2|^2/d_2)^2]$ can be obtained for the SWM1 process, where $G_\mathrm{B} = \mathrm{i}\, G_1 G_2 G_2 G_3 G_3'^*$, $d_2 = \mathrm{i}(\Delta_1 + \Delta_2) + \Gamma_{20}$. The intensity $I_\mathrm{SWM1} \propto |\rho_{10\mathrm{b}}^{(5)}|^2$. When no laser beam is blocked, SWM1 and SWM2 will form at the same time and interact with each other. As for the SWM2 formed with E_2 working as the outer dressing field (described as DSWM2), according to the dressed perturbation chain $\rho_{00}^{(0)} \xrightarrow{\omega_1} \rho_{(G_2\pm)0}^{(1)} \xrightarrow{-\omega_3} \rho_{30}^{(2)} \xrightarrow{\omega_3} \rho_{(G_2\pm G_4\pm)0}^{(3)} \xrightarrow{\omega_4} \rho_{40}^{(4)} \xrightarrow{-\omega_4} \rho_{10}^{(5)}$, we can obtain $\rho_{10\mathrm{Da}}^{(5)} = G_\mathrm{A}/[d_3 d_4 (d_1 + |G_2|^2/d_2)(d_1 + |G_2|^2/d_2 + |G_4|^2/d_4)^2]$, which is the expression for the DSWM2. The intensity $I_\mathrm{DSWM2} \propto |\rho_{10\mathrm{Da}}^{(5)}|^2$. Similarly, for the SWM1 formed with E_4 works as the outer dressing field (described as DSWM1), according to the dressed perturbation chain $\rho_{00}^{(0)} \xrightarrow{\omega_1} \rho_{(G_2\pm)0}^{(1)} \xrightarrow{\omega_2} \rho_{20}^{(2)} \xrightarrow{-\omega_2} \rho_{(G_2\pm G_4\pm)0}^{(3)} \xrightarrow{-\omega_3} \rho_{30}^{(4)} \xrightarrow{\omega_3} \rho_{10}^{(5)}$, we can obtain $\rho_{10\mathrm{Db}}^{(5)} = G_\mathrm{B}/[d_2 d_3 (d_1 + |G_4|^2/d_4)(d_1 + |G_2|^2/d_2 + |G_4|^2/d_4)^2]$, which is the expression for the DSWM1. The intensity $I_\mathrm{DSWM1} \propto |\rho_{10\mathrm{Db}}^{(5)}|^2$. The expressions of DSWM1 and DSWM2 reveal that the two SWMs are closely related to each other by the dressing effect. By adjusting the probe and the dressed field detuning, many interesting phenomena can be obtained.

3. Experimental results

In Fig. 2, curve 1 is the probe beam transmission with EIT windows and curve 2 is the measured SWM signals. The two absorption dips from left to right correspond to the hyperfine-level transitions from ^{85}Rb $|5S_{1/2},\ \mathrm{F} = 3\rangle$ to $|5P_{3/2},\ \mathrm{F} = 1, 2, 3\rangle$ and from ^{87}Rb $|5S_{1/2},\ \mathrm{F} = 2\rangle$ to $|5P_{3/2},\ \mathrm{F} = 0, 1, 2\rangle$, respectively. On one hand, in curve 1, there are two peaks on the absorption dips. The right one, which satisfies $\Delta_1 + \Delta_4 = 0$, is the EIT window created by the pump field E_4 in the system $|0\rangle - |1\rangle - |4\rangle$; the left one, which satisfies $\Delta_1 + \Delta_2 = 0$, is created by the dressing field E_2 in the system $|0\rangle - |1\rangle - |2\rangle$. On the other hand, in curve 2, the left peak of the pure SWM signal corresponding to the $|0\rangle - |1\rangle - |2\rangle$ EIT window is split due to the dressing effect of E_2, the right peak of the pure SWM signal corresponding to the $|0\rangle - |1\rangle - |4\rangle$ EIT window is split into two peaks due to the dressing effect of E_4.

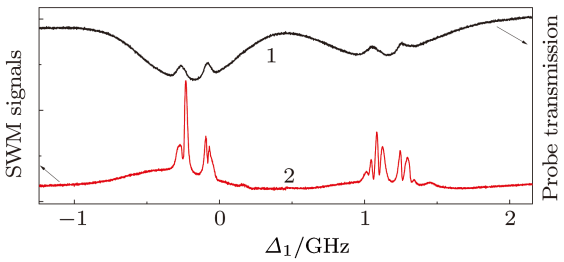


Fig. 2. (colour online) Curve 1 is the probe beam transmission with two EIT windows versus the probe detuning Δ_1. Curve 2 is the measured SWM signals. The experimental parameters are $G_1 = 4.6$ mW, $G_2 = 50$ mW, $G_3 = G_3' = 61$ mW, $G_4 = 30$ mW. The other parameters are $\Delta_2 = 0$ MHz, $\Delta_3 = 300$ MHz.

In the experiment, we measure the SWM signals versus the dressing field detuning Δ_2 for different probe detuning Δ_1 in the five-level atomic system. Generally, when no laser beam is blocked, two SWM signals will form simultaneously and interact with each other. The total SWM signals can be obtained and detected when we overlap the two SWM signals. We perform two groups of experiments with different intensities of the fields E_2 and E_4. The results of the first experiment group are shown in Fig. 3(a), where we make the intensity of the field E_2 large and the intensity of the field E_4 small. In Fig. 3(a), the curve 1 can be obtained when all the laser beams are open. There are three components, I_SWM2, I_DSWM1 and I_ESSWM2 in the total signals. The I_ESSWM2 represents the enhancement and suppression of SWM2 caused by the dressing field E_2 and

the quantum interference of E_2 in SWM2.[10] Because this experiment measures the signals versus the dressing field detuning Δ_2 for different probe detuning Δ_1, the general baseline is mainly caused by the field E_4, which represents SWM2 versus Δ_1. The general baseline is less obvious than the signals shown in Fig. 3(b). Double-peak Autler–Townes (AT) splitting in the general baseline caused by the self-dressing effect of the field E_4 with the AT splitting separation $2G_4$ forms the $\rho^{(5)}_{10\mathrm{Db}}$ approximately. The $|G_4+\rangle$ and the $|G_4-\rangle$ created by the field E_4 correspond to the left and the right peaks in the AT splitting, respectively. Moreover, peaks and dips on each baseline in the curve 1 of Fig. 3(a) include the combination of I_{DSWM1} and I_{ESSWM2}. Curve 2 of Fig. 3(a) represents I_{SWM1} with the laser beam E_4 blocked. Each peak of SWM1 also shows the AT splitting caused by the self-dressing effect of the field E_2. Due to the weak dressing effect of the field E_4, compared with I_{ESSWM2}, the suppression on SWM1 is so small that I_{DSWM1} is almost equal to I_{SWM1}. We can obtain the composition of I_{ESSWM2} and I_{ESSWM1} by subtracting the general baseline of the total signals and the SWM1, as shown in curve 4 of Fig. 3(a). Here, I_{ESSWM1} represents the enhancement and suppression of SWM1 caused by the dressing field E_4 and the quantum interference of E_4 in SWM1, i.e. I_{DSWM1}–I_{SWM1}. Because the intensity of E_4 is quite small, I_{ESSWM1} is small. Therefore, the signals in curve 4 mainly represent I_{ESSWM2} caused by E_2. According to the dressed-state theory, the dressed state energy levels $|G_2\pm\rangle$ created by the field E_2 can shift when scanning the detuning Δ_2. To be more specific, the suppression on SWM2 is strongest when the condition $\Delta_1 + \Delta_2 = 0$ is satisfied, because the field E_1 hits the virtual energy level caused by the field E_2. The SWM2 is enhanced when $\Delta_1 + \Delta_2 \pm G_2 = 0$ is satisfied. It is easy to see from curve 4 of Fig. 3(a) that when Δ_1 nearly satisfies $\Delta_1 + \Delta_2 = 0$, the suppression is the largest. At both sides of the curve, the enhancement is much stronger. By subtracting SWM2 from the total signals in curve 1 of Fig. 3(a), we can obtain the composition of quantum interference effects I_{ESSWM2} and I_{DSWM1} as shown in curve 3 of Fig. 3(a). Because E_4 is small, I_{SWM2} is quite small. Therefore, curve 3 is quite similar to curve 1 in Fig. 3(a).

In the second experiment group, we make the intensity of the field E_4 larger than that in the first group and keep the intensity of E_2 the same as that in the former experiment. Figure 3(b) represents the measured total signals versus the dressing field detuning Δ_2 for different probe detuning Δ_1. Comparing curve 1 of Fig. 3(a) with Fig. 3(b), we can see that the effect of I_{ESSWM1} becomes much more obvious due to the stronger intensity of the field E_4. For example, the signals show dips that do not appear in curve 1 of Fig. 3(a), because E_4 is so small in the first experiment group that the suppression on SWM2 can almost be ignored. Moreover, the depth of the dips in Fig. 3(b) is much larger than those in curve 1 of Fig. 3(a). Since there are two SWM signals in the system, when scanning the dressing field detuning, both I_{DSWM1} and I_{ESSWM2} are obtained simultaneously. The combination of I_{DSWM1} and I_{ESSWM2} makes suppression shapes in the experiment, as shown in Fig. 3(b). The dashed curve in Fig. 3(b) is the profile of the double-peak SWM signal versus Δ_1.

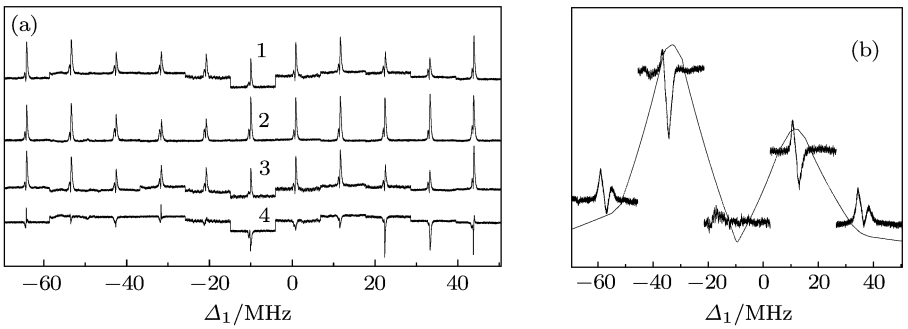


Fig. 3. (a) Curve 1–4 SWM signals obtained by scanning Δ_2 for different Δ_1. The powers of the laser beams are 3.7 mW (E_1), 26.6 mW (E_2), 46.1 mW ($E_3 + E_3'$) and 3.6 mW (E_4). Curve 1 signals were obtained with all laser beams open; curve 2 signals were obtained with the laser beam E_4 blocked; curve 3 is the sum of I_{ESSWM2} (enhancement and suppression of SWM2 caused by the field E_2 without the effect of E_4) and I_{DSWM1} (SWM1 outer dressed by E_4); curve 4 is the sum of I_{ESSWM2} and I_{ESSWM1}. (b) Measured SWM signals. The powers of the laser beams are 3.9 mW (E_1), 26.6 mW (E_2), 41 mW ($E_3 + E_3'$) and 50 mW (E_4). The curves are signals obtained with all laser beams on. The dashed curve is the profile of the double-peak SWM signal versus Δ_1. The other parameters are $\Delta_2 = 0$ MHz, $\Delta_3 = 300$ MHz.

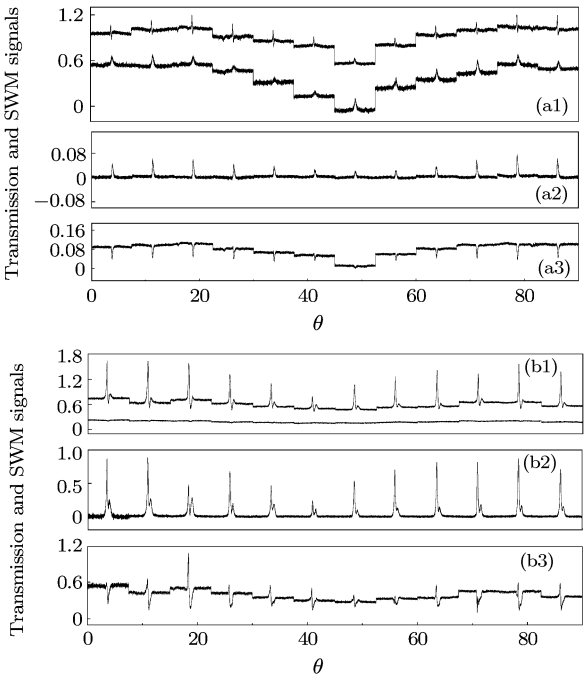


Fig. 4. (a1), (b1) Polarization dependence of the measured SWM signals (the upper curve) and probe transmission signals (the lower curve) by scanning Δ_2 with all laser beams on. (a2), (b2) The measured SWM signals with the laser beam E_4 blocked. (a3), (b3) The difference of the upper curve 1 and the (a2) and (b2) versus rotation angle θ (increases from 0° to 90° with a variation step of 8°). The experimental parameters in (a) are 3.7 mW (E_1), 5.6 mW (E_2), 15.5 mW ($E_3 + E_3'$) and 67 mW (E_4). The experimental parameters in (b) are 3.7 mW (E_1), 28 mW (E_2), 44 mW ($E_3 + E_3'$), 16 mW (E_4). The other parameters are $\Delta_2 = 0$ MHz, $\Delta_3 = 300$ MHz.

In the following experiment, we show the polarization properties of the enhancement and suppression of two coexisting SWM processes in multi-Zeeman level atomic system by changing the polarization of the probe beam.[3] Here, we set Δ_1 far away from the region of half suppression and half enhancement. Figure 4 presents the probe transmission signals and the SWM signals when scanning the dressing field detuning Δ_2 from $\theta = 0°$ to $\theta = 90°$ with a step of 8°, where θ is the polarization angle of the probe field E_1. In the experiment, of which the result is shown in Fig. 4(a1), we make the intensity of the field E_2 small and the intensity of the field E_4 large. The upper curve shows the signal intensity, which consists mainly of the SWM signals $I_{\rm SWM2}$, $I_{\rm DSWM1}$ and $I_{\rm ESSWM2}$ with all beams on. Here, the baseline of each θ of the upper curve consists of SWM2. The peaks and the dips in the upper curve are the superposition of $I_{\rm DSWM1}$ and $I_{\rm ESSWM2}$. The lower curve is the corresponding probe transmission signals versus the dressing field detuning Δ_2. Therefore the baseline of each θ of the lower curve is the pure transmitted probe field intensity and the EIT phenomenon. Because of the splitting of the level $|1\rangle$, the probe field is no longer absorbed when the condition $\Delta_1 = -\Delta_2$ is satisfied. It is difficult to obtain any pure SWM signal with all the beams on. When we block E_4 beam, Fig. 4(a2) shows the signal intensity that only consists of $I_{\rm SWM1}$. By subtracting the signals in Fig. 4(a2) from the signals in Fig. 4(a1), one can obtain the composition of quantum interference effects $I_{\rm ESSWM1}$ and $I_{\rm ESSWM2}$, as shown in Fig. 4(a3).

In Fig. 4(a), E_2 is quite small, so figure 4(a3) mainly shows the suppression caused by E_4. The amplitude of the suppression of the curve gets smaller with the increase of θ from 0° to 45°. In Fig. 4(b), E_2 is larger, so Fig. 4(b3) shows the suppression caused by E_4 and the effect of enhancement and suppression cause by E_2. We can also find that the amplitude of the suppression and enhancement of the curve also gets smaller with the increase of θ from 0° to 45°. These phenomena can be explained by the total linear, right hand and left hand circularly polarized SWM expression as

$$\rho_{\rm S2}^{(5)0} = \sum_{M=2,1,-1,-2} \mathrm{i}\, G_{1_M}^0 G_3^0 (G'^0_3)^* (G_4^0)^2 \Bigg/ \Bigg\{ \Bigg[\Gamma_{1_M 0_M} + \mathrm{i}\,\Delta_1 + \frac{(G_2^0)^2}{\Gamma_{2_M 0_M} + \mathrm{i}(\Delta_1 + \Delta_2) + \dfrac{(G_{1_M}^0)^2}{\Gamma_{2_M 1_M} + \mathrm{i}\,\Delta_2}} + \frac{(G_4^0)^2}{\Gamma_{4_M 0_M} + \mathrm{i}(\Delta_1 + \Delta_4) + \dfrac{(G_{1_M}^0)^2}{\Gamma_{4_M 1_M} + \mathrm{i}\,\Delta_4}} \Bigg]^3 [\Gamma_{3_M 0_M} + \mathrm{i}(\Delta_1 - \Delta_3)]\,[\Gamma_{4_M 0_M} + \mathrm{i}(\Delta_1 + \Delta_4)] \Bigg\}, \quad (1)$$

$$\rho_{\rm S2}^{(5)+} = \sum_{M=-2}^{2} \mathrm{i}\, G_{1_M}^+ G_3^0 (G'^0_3)^* (G_4^0)^2 \Bigg/ \Bigg\{ \Bigg[\Gamma_{1_M 0_{M-1}} + \mathrm{i}\,\Delta_1 + \frac{(G_2^0)^2}{\Gamma_{2_M 0_{M-1}} + \mathrm{i}(\Delta_1 + \Delta_2) + \dfrac{(G_{1_M}^+)^2}{\Gamma_{2_M 1_M} + \mathrm{i}\,\Delta_2}} + \frac{(G_4^0)^2}{\Gamma_{4_M 0_{M-1}} + \mathrm{i}(\Delta_1 + \Delta_4) + \dfrac{(G_{1_M}^+)^2}{\Gamma_{4_M 1_M} + \mathrm{i}\,\Delta_4}} \Bigg]^3 \big[\Gamma_{3_M 0_{M-1}} + \mathrm{i}(\Delta_1 - \Delta_3)\big]\,\big[\Gamma_{4_M 0_{M-1}} + \mathrm{i}(\Delta_1 + \Delta_4)\big] \Bigg\}, \quad (2)$$

$$\rho_{\rm S2}^{(5)-} = \sum_{M=-2}^{2} \mathrm{i}\, G_{1_M}^{-} G_3^0 (G'^0_3)^* (G_4^0)^2 \Big/ \Bigg\{ \Bigg[\Gamma_{1_M 0_{M-1}} + \mathrm{i}\,\Delta_1 + \frac{(G_2^0)^2}{\Gamma_{2_M 0_{M-1}} + \mathrm{i}(\Delta_1+\Delta_2) + \dfrac{(G_{1_M}^{-})^2}{\Gamma_{2_M 1_M} + \mathrm{i}\,\Delta_2}} + \frac{(G_4^0)^2}{\Gamma_{4_M 0_{M+1}} + \mathrm{i}(\Delta_1+\Delta_4) + \dfrac{(G_{1_M}^{-})^2}{\Gamma_{4_M 1_M} + \mathrm{i}\,\Delta_4}} \Bigg]^3 \left[\Gamma_{3_M 0_{M+1}} + \mathrm{i}(\Delta_1 - \Delta_3)\right] \left[\Gamma_{4_M 0_{M+1}} + \mathrm{i}(\Delta_1+\Delta_4)\right] \Bigg\}, \quad (3)$$

In Eqs. (1), (2), and (3), $(G_2^0)^2$ can control the enhancement and suppression of SWM2 caused by the dressing field E_2. When θ gets closer to 45°, the dressing effect of $(G_{1_M}^{\pm})^2$ gets bigger than that of $(G_{1_M}^{0})^2$. This difference is caused by Clebsch–Gordan (CG) coefficients, which are related to various transitions between Zeeman sublevels in all pathways when analyzing the dressing effect. The Rabi frequencies are different even with the same laser field, because the CG coefficients can be different for different transitions between Zeeman sublevels. Considering the CG coefficients, we can obtain $|G_1^{\pm}|^2 = 5|G_1^0|^2/2$. This effect will diminish the influence of $(G_2^0)^2$. Therefore, the peaks become smaller.

Compared to the former experiment group, we only increase the intensity of the field E_2 to observe the influence of the dressing effect of E_2 on SWM signals. By comparing the upper curves in Figs. 4(a1) and 4(b1), it can be seen that the peak of the signal at $\theta = 0°$ in Fig. 4(b) gets big. This is because the component $I_{\rm SWM2}$ in the upper curve of Fig. 4(a1) is smaller than that of Fig. 4(b1) due to the dressing effect of E_2. On the other hand, by comparing Figs. 4(a3) and 4(b3), it can be seen that when E_2 is small, the enhancement and suppression on SWM2 is smaller.

4. Conclusion

In summary, we report the dependences of the SWM signals in the EIT windows on the frequency detuning based on theoretical analysis of the enhancement and suppression in two mutual dressing SWM processes. We demonstrate the evolutions of the enhancement and suppression of the signals caused by external dressing effect by scanning one dressing field at different probe field detunings. We observe polarization dependence of the enhancement and suppression of the SWM signals.

References

[1] Harris S E 1997 *Phys. Today* **50** 36

[2] Gea-Banacloche J, Li Y Q, Jin S Z and Xiao M 1995 *Phys. Rev.* A **51** 576

[3] Ling H Y, Li Y Q and Xiao M 1996 *Phys. Rev.* A **53** 1014

[4] Wang B, Xiao Y J, Yang X, Xie C, Wang H and Xiao M 2006 *Opt. Lett.* **31** 3647

[5] Li S, Wang B, Yang X, Han Y, Wang H, Xiao M and Peng K C 2006 *Phys. Rev.* A **74** 033821

[6] Wu Y and Deng L 2004 *Phys. Rev. Lett.* **93** 143904

[7] Wu Y, Saldana J and Zhu Y F 2003 *Phys. Rev.* A **67** 013811

[8] Li P Z, Nie Z Q, Zhang Y P, Jiang T, Du Y G, Gan C L, Song J P and Lu K Q 2009 *Chin. Phys. Lett.* **24** 3420

[9] Li C S, Yin W T, Yuan C Z, Shi M Z, Zhao Y and Zhang Y P 2009 *Chin. Phys. Lett.* **26** 064204

[10] Li C B, Zhang Y P, Nie Z Q, Du Y G, Wang R M, Song J P and Xiao M 2010 *Phys. Rev.* A **81** 033801

[11] Li C B, Zhang Y P, Nie Z Q, Zheng H B, Shi M Z, Liu D N, Song J P and Lu K Q 2009 *Chin. Phys.* B **18** 535408

[12] Zhu C J, Senin A A, Lu Z H, Gao J, Xiao Y and Eden J G 2005 *Phys. Rev.* A **72** 023811

[13] Magno W C, Prandini R B, Nussenzveig P and Vianna S S 2001 *Phys. Rev.* A **63** 063406